Electronic Supplementary Material (ESI) for Nanoscale Horizons.

Supplementary Materials for

Multiplexed molecular imaging with surface enhanced resonance Raman scattering nanoprobes reveals immunotherapy response in mice via multichannel image segmentation

Authors:
Chrysafis Andreou[1,2,3*], Konstantinos Plakas[4†], Naxhije Berisha[1,5†], Mathieu Gigoux[6], Lauren E. Rosch[4], Rustin Mirsafavi[1], Anton Oseledchyk[1], Suchetan Pal[1], Dmitriy Zamarin[6], Taha Merghoub[6], Michael R. Detty[4], Moritz F. Kircher[7,8]

Affiliations:
[1] Department of Radiology, Memorial Sloan Kettering Cancer Center, 1275 York Avenue, New York, New York 10065, USA
[2] Center for Molecular Imaging and Nanotechnology (CMINT), Memorial Sloan Kettering Cancer Center, New York, NY 10065, USA
[3] Department of Electrical and Computer Engineering, University of Cyprus, Nicosia, 1678 Nicosia, Cyprus
[4] Department of Chemistry, University at Buffalo, The State University of New York, Buffalo, New York 14260-3000, USA
[5] Department of Chemistry, The Graduate Center of the City University of New York, New York, NY 10016 USA
[6] Department of Immunology, Memorial Sloan Kettering Cancer Center, 1275 York Avenue, New York, New York 10065, USA
[7] Department of Imaging, Dana-Farber Cancer Institute and Harvard Medical School, Boston, MA 02215, USA
[8] Department of Radiology, Brigham & Women's Hospital and Harvard Medical School, Boston, MA 02215, USA

*Correspondence to: andreou.chrysafis@ucy.ac.cy

†These authors contributed equally

This PDF file includes:

Materials and Methods

Synthesis of:

ChPIR-728

(*E*)-4-(4-(dimethylamino)styryl)-2,6-di(thien-2-yl)thiopyrylium hexafluorophosphate.

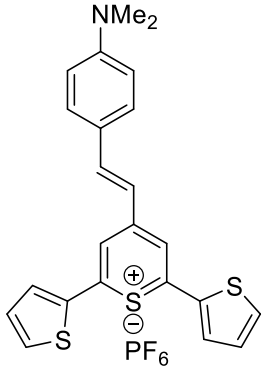

4-Methyl-2,6-di(thien-2-yl)thiopyrylium hexafluorophosphate[1] (50.0 mg, 0.119 mmol), 4-(dimethylamino)benzaldehyde (18.9 mg, 0.127 mmol) and acetic anhydride (0.82 mL) were heated at 105˚C for 10 min in a test tube. The reaction mixture was then cooled to ambient temperature. Acetonitrile (0.25 mL) was added, and the mixture cooled on ice for 15 min. The mixture was then filtered to afford 65.6 mg (79%) of a metallic green solid, m.p. 221-222 ˚C; ^{1}H NMR [500 MHz, CD_2Cl_2] δ 8.10 (d, 1 H, J = 15.0 Hz), 7.99 (s, 2 H), 7.86 (d, 4 H, J = 4.0 Hz), 7.75 (d, 2 H, J = 8.5 Hz), 7.29 (t, 2 H, J = 4.0 Hz), 7.15 (d, 1 H, J = 15.5 Hz), 6.84 (d, 2 H, J = 8.0 Hz), 3.21 (s, 6 H); λ_{max} (CH_2Cl_2) 728 nm (ε = 5.8 × 10^4 $M^{-1}cm^{-1}$); IR (ATR) 1612.3 cm^{-1} (m, C=C), 1523.1 cm^{-1} (m, aromatic C=C), 1332.2 cm^{-1} (m, C-N); HRMS (ESI) *m/z* 406.0760 (calcd for $C_{23}H_{20}N_1S_3^+$: 406.0752).

ChPIR-732

(*E*)-4-(4-(dimethylamino)styryl)-2,6-di(selenophen-2-yl)thiopyrylium hexafluorophosphate.

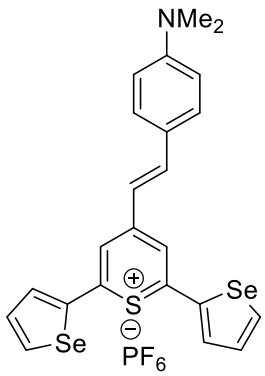

4-Methyl-2,6-di(selenophen-2-yl)thiopyrylium hexafluorophosphate[2] (50.0 mg, 0.097 mmol), 4-(dimethylamino)benzaldehyde (16.0 mg, 0.107 mmol) and acetic anhydride (0.70 mL) were heated at 105˚C for 10 min in a test tube. The reaction mixture was then cooled to ambient temperature. Acetonitrile (0.20 mL) was added, and the mixture cooled on ice for 15 min. The mixture was then filtered to afford 35.7 mg (57%) of a metallic green solid, m.p. >260 ˚C; ^{1}H NMR [500 MHz, CD_2Cl_2] δ 8.50 (d, 2 H, J = 5.5 Hz), 8.10 (d, 1 H, J = 15.0 Hz), 8.05 (d, 2 H, J = 4.0 Hz), 7.93 (s, 2 H), 7.80 (d, 2 H, J = 3.50 Hz), 7.54 (t, 2 H, J = 4.0 Hz), 7.19 (d, 1 H, J = 15.0 Hz), 6.85 (d, 2 H, J = 8.0 Hz) 3.23 (s, 6 H); λ_{max} (CH_2Cl_2) 732 nm ε = 3.5 × 10^4 $M^{-1}cm^{-1}$); HRMS (ESI) *m/z* 501.9654 (calcd for $C_{23}H_{20}N_1S_1{}^{80}Se_2^+$: 501.9641).

ChPIR-768

(*E*)-4-(4-(dimethylamino)styryl)-2,6-di(selenophen-2-yl)selenopyrylium hexafluorophosphate.

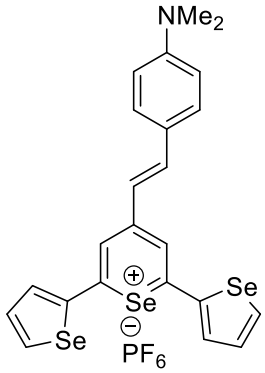

4-Methyl-2,6-di(selenophen-2-yl)selenopyrylium hexafluorophosphate (30.0 mg, 0.052 mmol), 4-(dimethylamino)benzaldehyde (8.50 mg, 0.057 mmol) and acetic anhydride (0.36 mL) were heated at 105˚C for 5 min in a test tube. The reaction mixture was then cooled to ambient temperature. Acetonitrile (0.10 mL) was added, and the mixture cooled on ice for 15 min. The mixture was then filtered to afford 17.2 mg (47%) of a metallic green solid, m.p. >260 ˚C; ^{1}H NMR [500 MHz, CD_2Cl_2] δ 8.51 (d, 2 H, J = 5.5 Hz), 8.14 (d, 2 H, J = 15.0 Hz), 7.90 (s, 2 H), 7.88 (s, 2 H), 7.80 (d, 2 H, J = 8.0 Hz), 7.53 (s, 2 H, J = 4.0 Hz), 7.27 (d, 1 H, J = 15.0 Hz), 6.88 (d, 2 H, J = 8.5 Hz), 3.24 (s, 6 H); λ_{max} (CH_2Cl_2) 768 nm (ε = 4.1 × 10^4 $M^{-1}cm^{-1}$); HRMS (ESI) *m/z* 547.9104 (calcd for $C_{23}H_{20}N_1{}^{80}Se_3^+$: 547.9094).

ChPIR-761

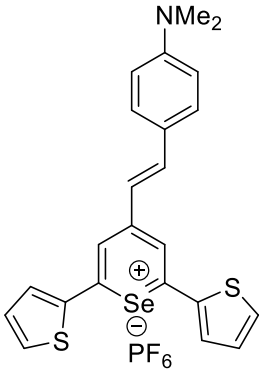

(*E*)-4-(4-(dimethylamino)styryl)-2,6-di(thien-2-yl)selenopyrylium hexafluorophosphate.
4-Methyl-2,6-di(thien-2-yl)selenopyrylium hexafluorophosphate (50.0 mg, 0.107 mmol), 4-(dimethylamino)benzaldehyde (17.0 mg, 0.114 mmol) and acetic anhydride (0.75 mL) were heated at 105˚C for 5 min in a test tube. The reaction mixture was then cooled to ambient temperature. Acetonitrile (0.22 mL) was added, and the mixture cooled on ice for 15 min. The mixture was then filtered to afford 38.9 mg (61%) of a metallic green solid, m.p. 224-226 ˚C; ^{1}H NMR [500 MHz, CD_2Cl_2] δ 8.15 (d, 2 H, J = 15.0 Hz), 7.96 (s, 1 H), 7.79 (t, 4 H, J = 5.0 Hz), 7.72 (d, 2 H, J = 3.5 Hz), 7.30 (t, 2 H, J = 4.0 Hz), 7.22 (d, 1 H, J = 14.5 Hz), 6.87 (d, 2 H, J = 9.0 Hz), 3.22 (s, 6 H);); λ_{max} = (CH_2Cl_2) 761 nm ε = 4.0 × 10^4 $M^{-1}cm^{-1}$; IR (ATR) 1613.3 cm^{-1} (m, C=C), 1510.8 cm^{-1} (m, aromatic C=C) 1330.8 cm^{-1} (m, C-N); HRMS (ESI) 454.0294 (calcd for $C_{23}H_{20}N_1S_2{}^{80}Se_1{}^+$: 454.0246).

ChPIR-817

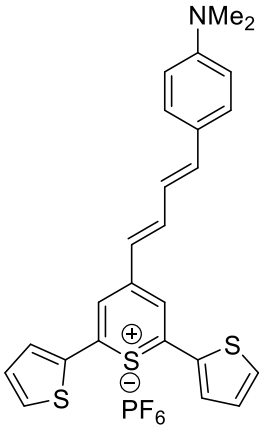

4-((1*E*,3*E*)-4-(4-(dimethylamino)phenyl)buta-1,3-dien-1-yl)-2,6-di(thien-2-yl)thiopyrylium hexafluorophosphate.
4-Methyl-2,6-di(thien-2-yl)thiopyrylium hexafluorophosphate[1] (50.0 mg, 0.119 mmol), 4-(dimethylamino)cinnamaldehyde (22.3 mg, 0.127 mmol) and acetic anhydride (1.23 mL) were heated at 105˚C for 10 min in a test tube. The reaction mixture was then cooled to ambient temperature. Acetonitrile (0.25 mL) was added, and the mixture cooled on ice for 15 min. The mixture was then filtered to afford 65.6 mg (79%) of a metallic green solid, m.p. 204-206 ˚C; ^{1}H NMR [500 MHz, CD_2Cl_2] δ 8.03 (t, 1 H, J = 14.0 Hz), 7.86 (s, 2 H), 7.78 (m, 4 H), 7.63 (d, 2 H), 7.52 (d, 2 H, J = 14.5 Hz), 7.31 (t, 2 H, J = 4.0 Hz), 7.17 (t, 1 H, J = 14.5 Hz), 6.79 (d, 2 H, J = 8.5 Hz), 6.74 (d, 2 H, J = 15.0 Hz), 3.09 (s, 6 H); λ_{max} (CH_2Cl_2) 817 nm (ε = 6.5 × 10^4 $M^{-1}cm^{-1}$); IR (ATR) 1614.0 cm^{-1} (s, C=C), 1505.0 cm^{-1}.(m, aromatic C=C), 1374.6 cm^{-1} (m, C-N); HRMS (ESI) *m/z* 432.0925 (calcd for $C_{25}H_{22}N_1S_3{}^+$: 432.0909).

ChPIR-820[4]

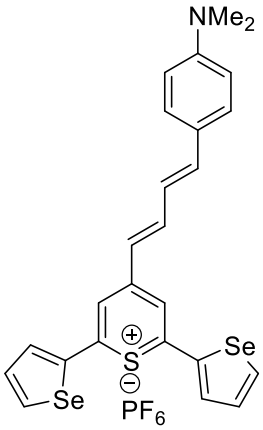

4-((1*E*,3*E*)-4-(4-(dimethylamino)phenyl)buta-1,3-dien-1-yl)-2,6-di(selenophen-2-yl)thiopyrylium hexafluorophosphate.
4-Methyl-2,6-di(selenophen-2-yl)thiopyrylium hexafluorophosphate[2] (50.0 mg, 0.097 mmol), 4-(dimethylamino)benzaldehyde (16.0 mg, 0.107 mmol) and acetic anhydride (1.00 mL) were heated at 105 ˚C for 10 min in a test tube. The reaction mixture was then cooled to ambient temperature. Acetonitrile (0.20 mL) was added, and the mixture cooled on ice for 15 min. The mixture was then filtered to afford 35.7 mg (57%) of a metallic green solid, m.p. >260 ˚C: ^{1}H NMR [500 MHz, CD_2Cl_2] δ 8.57 (d, 1 H, J = 5.0 Hz), 8.16-8.12 (m, 2 H), 8.03 (d, 2 H, J = 3.0 Hz), 7.91 (s, 2 H), 7.59 (d, 2 H, J = 9.0 Hz), 7.52 (t, 2 H, J = 4.5 Hz), 7.42 (d, 1 H, J = 14.5 Hz), 7.18-7.13 (m, 2 H), 6.78 (d, 2 H, J = 9.0 Hz), 6.74 (s, 1 H), 3.18 (s, 6 H); λ_{max} (CH_2Cl_2) 820 nm (ε = 4.5 × 10^4 $M^{-1}cm^{-1}$); IR (ATR) 1604.6 cm^{-1} (m, C=C), 1504.6 cm^{-1} (m, aromatic C=C), 1377.2 (m, C-N); HRMS (ESI) *m/z* 527.9808 (calcd for $C_{25}H_{22}N_1S_1{}^{80}Se_2{}^+$: 527.9798).

ChPIR-863

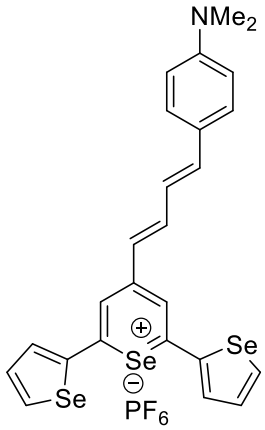

4-((1*E*,3*E*)-4-(4-(dimethylamino)phenyl)buta-1,3-dien-1-yl)-2,6-di(selenophen-2-yl)selenopyrylium hexafluorophosphate.

4-Methyl-2,6-di(selenophen-2-yl)selenopyrylium hexafluorophosphate (50.0 mg, 0.089 mmol), 4-(dimethylamino)cinnamaldehyde (16.7 mg, 0.095 mmol) and acetic anhydride (1.00 mL) were heated at 105˚C for 5 min in a test tube. The reaction mixture was then cooled to ambient temperature. Acetonitrile (0.20 mL) was added, and the mixture cooled on ice for 15 min. The mixture was then filtered to afford 27.3 mg (40%) of a metallic red solid, m.p. >260 ˚C; ^{1}H NMR [500 MHz, CD_2Cl_2] δ 8.57 (d, 1 H, J = 5.0 Hz), 8.13 (m, 1 H), 8.03 (d, 2 H, J = 3.0 Hz), 7.91 (s, 1 H), 7.59 (d, 2 H, J = 9.0 Hz) 7.52(m, 2 H), 7.42 (d, 1 H, J = 14.5 Hz), 7.15 (m, 2 H), 6.78 (d, 2 H, J = 9.0 Hz), 6.74 (s, 1 H), 3.11 (s, 6 H); IR (ATR), 1611.2 cm^{-1} (s, C=C) 1496.9 cm^{-1} (m, aromatic C=C), 1380.4 (m, C-N); λ_{max} (CH_2Cl_2) 863 nm (ε=3.7 × 10^4 M^{-1}cm^{-1}). HRMS (ESI) *m/z* 573.9238 (calcd for $C_{25}H_{22}N_1{}^{80}Se_3{}^+$: 573.9250).

ChPIR-853

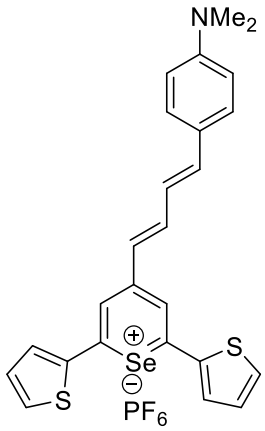

4-((1*E*,3*E*)-4-(4-(dimethylamino)phenyl)buta-1,3-dien-1-yl)-2,6-di(thien-2-yl)selenopyrylium hexafluorophosphate.

4-Methyl-2,6-di(thien-2-yl)selenopyrylium hexafluorophosphate (50.0 mg, 0.097 mmol), 4-(dimethylamino)cinnamaldehyde (18.2 mg, 0.0.104 mmol) and acetic anhydride (1.00 mL) were heated at 105˚C for 5 min in a test tube. The reaction mixture was then cooled to ambient temperature. Acetonitrile (0.22 mL) was added, and the mixture cooled on ice for 15 min. The mixture was then filtered to afford 33.8 mg (52%) of a metallic green solid, m.p. > 260 ˚C: [500 MHz, CD_2Cl_2] δ 8.51-8.49 (m, 1 H), 8.04 (d, 1 H, J = 12.0 Hz), 7.97 (br s, 2 H), 7.84 (br s, 3 H), 7.59-5.58 (m, 2 H), 7.50-7.45 (m, 3 H), 7.17-7.12 (m, 2 H), 6.76-6.72 (m, 2 H), 3.28 (s, 6 H); λ_{max} (CH_2Cl_2) 853 nm (ε = 3.7 × 10^4 M^{-1}cm^{-1}). IR (ATR) 1611.7 cm^{-1} (s, C=C) 1504.4 cm^{-1} (m, aromatic C=C), 1396.3 cm^{-1} (m, C-N); HRMS (ESI) *m/z* 480.0335 (calcd for $C_{25}H_{22}N_1S_2{}^{80}Se_1{}^+$: 480.0353).

ChPIR-813

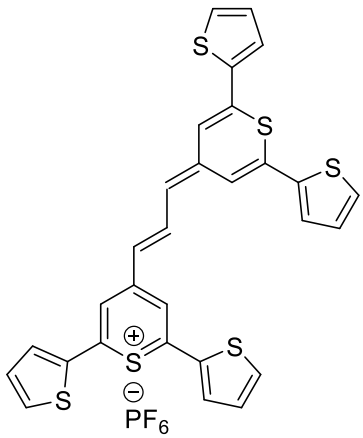

(*E*)-4-(3-(2,6-di(thien-2-yl)-4H-thiopyran-4-ylidene)prop-1-en-1-yl)-2,6-di(thien-2-yl)thiopyrylium hexafluorophosphate.

4-Methyl-2,6-di(thien-2-yl)thiopyrylium hexafluorophosphate (50.0 mg, 0.119 mmol), 2-(2,6-di(thien-2-yl)-4H-thiopyran-4-ylidene)acetaldehyde (39.6 mg, 0.131 mmol) were dissolved in acetic anhydride (2.0 mL) and heated at 105 °C for 15 min. The reaction mixture was then cooled to ambient temperature. The reaction mixture was then filtered and the solid residue was rinsed with diethyl ether to yield 71.3 mg (85%) of a metallic red solid, m.p. > 260 °C; ^{1}H NMR [500 MHz, CD_2Cl_2] δ 920 (t, 1 H, J = 13.0 Hz), 8.70 (br, s, 2 H), 8.40 (br, s 2 H), 7.50-7.39 (m, 8 H), 7.07 (t, 4 H, J = 4.5 Hz), 6.58 (d, 2 H, J = 13.0 Hz); λ_{max} (CH_2Cl_2) 813 nm (ε = 2.8 × 10^5 M^{-1}cm^{-1}); HRMS (ESI) *m/z* 558.9805 (calcd for $C_{29}H_{19}S_6$: 558.9806). Anal. (cald for $C_{29}H_{19}S_6PF_6$: C, 49.42; H, 2.72. Found: C, 49.19; H, 2.79.

ChPIR-825

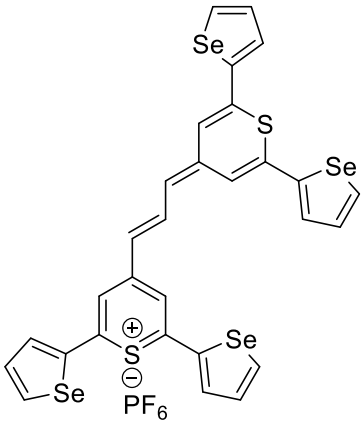

(*E*)-4-(3-(2,6-di(selenophen-2-yl)-4*H*-thiopyran-4-ylidene)prop-1-en-1-yl)-2,6-di(selenophen-2-yl)thiopyrylium hexafluorophosphate.

Prepared according to reference 2. 4-Methyl-2,6-di(selenophen-2-yl)thiopyrylium hexafluorophosphate (62.8 mg, 0.158 mmol), 2-(2,6-di(thiophen-2-yl)-4*H*-thiopyran-4-ylidene)acetaldehyde (74.0 mg, 0.144 mmol) and acetic anhydride (2.42 mL) were heated at 105 ˚C for 15 min in a test tube. The mixture was then cooled to ambient temperature., acetonitrile (1.0 mL) was added, and ether was used to precipitate the product. The product was collected by filtration to yield 95.0 mg (74%) of bronze solid, m.p. 249-250 ˚C: ^{1}H NMR [500 MHz, CD_3CN] δ 8.51-8.46 (m, 5 H), 7.88 (d, 4 H J = 3.0 Hz) 7.71 (br s, 4 H), 7.46(t, 4 H, J = 4.5 H), 6.62 (d, 2 H, J = 13.0 Hz); λ_{max} (CH_2Cl_2) 825 nm (ε = 2.3 × 10^5 $M^{-1}cm^{-1}$); 750 nm (ε = 5.2 × 10^4 $M^{-1}cm^{-1}$); 490 nm (ε = 2.8 × 10^4 $M^{-1}cm^{-1}$); IR (ATR) 1470.8 cm^{-1} (m, aromatic C=C). HRMS (ESI) *m/z* 750.7560 (calc for $C_{29}H_{19}S_2{}^{80}Se_4^+$: 750.7584). Anal. Calcd for $C_{29}H_{19}S_2Se_4PF_6$: C, 39.03; H, 2.15. Found: C, 39.28; H, 2.19.

ChPIR-870

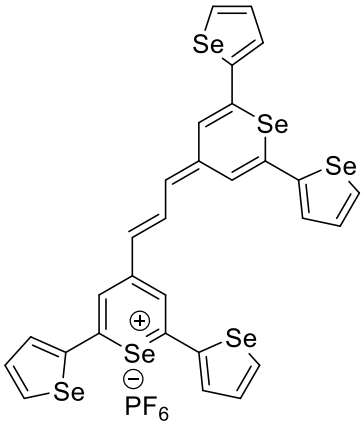

(*E*)-4-(3-(2,6-di(selenophen-2-yl)-4*H*-selenopyran-4-ylidene)prop-1-en-1-yl)-2,6-di(selenophen-2-yl)selenopyrylium hexafluorophosphate.

4-Methyl-2,6- di(selenophen-2-yl)selenopyrylium hexafluorophosphate (57.8 mg, 0.103 mmol), 2-(2,6-di(selenophen-2-yl)-4*H*-selenopyran-4-ylidene)acetaldehyde (50.0 mg, 0.113 mmol) and acetic anhydride (1.80 mL) were heated at 105 ˚C for 5 min in a test tube. The reaction mixture was then cooled to ambient temperature, acetonitrile (1.0 mL) was added, and ether was used to precipitate the product. The product was collected by filtration to yield 54.9 mg (54%) of a bronze solid, m.p. > 260 ˚C: ^{1}H NMR [500 MHz, CD_2Cl_2] δ 8.54 (t, 1 H, J = 13.5 Hz), 7.88 (d 4 H J = 3.0 Hz) 8.42 (d, 4 H, J = 5.5 Hz), 7.80 (d, 4 H, J = 4.0 H), 7.71 (br s, 4 H) 7.47-7.45 (m, 4 H), 6.75 (d, 2 H, J = 13.5 Hz); λ_{max} (CH_2Cl_2) 872 nm (ε = 2.2 × 10^5 $M^{-1}cm^{-1}$); 787 nm (ε = 4.6 × 10^4 $M^{-1}cm^{-1}$). IR (ATR) 1470.3 cm^{-1} (m, aromatic C=C); HRMS (ESI) *m/z* 846.6510 (calc for $C_{29}H_{19}{}^{80}Se_6^+$: 846.6472). Anal calcd for $C_{29}H_{19}Se_6PF_6$: C, 35.32; H, 1.94. Found: C, 35.58; H, 2.08.

ChPIR-794

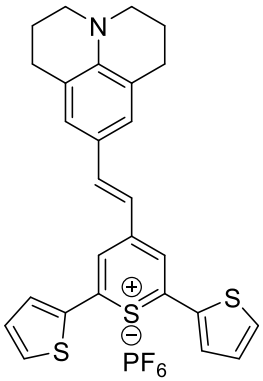

(*E*)-4-(2-(2,3,6,7-tetrahydro-*1H,5H*-pyrido[3,2,1-ij]quinolin-9-yl)vinyl)-2,6-di(thien-2-yl)thiopyrylium hexafluorophosphate.

4-Methyl-2,6-di(thien-2-yl)thiopyrylium hexafluorophosphate[1] (50.0 mg, 0.119 mmol) and 2,3,6,7-tetrahydro-*1H,5H*-pyrido[3,2,1-ij]quinoline-9-carbaldehyde (35.9 mg, 0.179 mmol) were dissolved in acetic anhydride (1.00 mL) and heated at 105 °C for 15 min in a test tube. The reaction mixture was cooled to ambient temperature precipitating a solid. The solid was collected by filtration and rinsed with diethyl ether to yield 61.1 mg (85%) of a metallic green solid, m.p. 200-201 °C; ^{1}H NMR [500 MHz, CD_2Cl_2] δ 7.87 (d, 1 H, J = 17.5 Hz), 7.75 (s, 2 H), 7.70 (d, 2 H, J = 6.5 Hz), 7.38 (s, 2 H), 7.27 (t, 2 H, J = 5.0 Hz), 7.01 (d, 1 H, J = 18.5 Hz), 3.53 (t, 4 H, J = 5.5 Hz), 2.81 (t, 4 H, J = 6.0 Hz), 2.05 (t, 4 H, J = 6.0 Hz); λ_{max} (CH_2Cl_2) 794 nm (ε = 8.90 × 10^4 $M^{-1}cm^{-1}$), 718 nm (ε = 5.60 × 10^4 $M^{-1}cm^{-1}$). HRMS (ESI) *m/z* 458.1067 (calcd for $C_{27}H_{24}NS_3$: 458.1065).

ChPIR-820$_2$

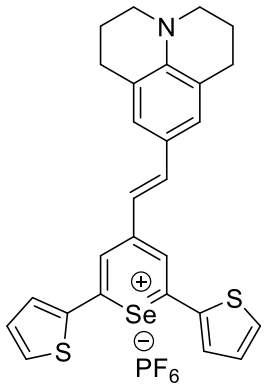

(*E*)-4-(2-(2,3,6,7-tetrahydro-*1H,5H*-pyrido[3,2,1-ij]quinolin-9-yl)vinyl)-2,6-di(thiophen-2-yl)selenopyrylium hexafluorophosphate

4-Methyl-2,6-di(thien-2-yl)selenopyrylium hexafluorophosphate (50.0 mg, 0.119 mmol) and 2,3,6,7-tetrahydro-*1H,5H*-pyrido[3,2,1-ij]quinoline-9-carbaldehyde (35.9 mg, 0.179 mmol) were dissolved in acetic anhydride (1.00 mL) and heated at 105 °C for 5 min in a test tube. The reaction mixture was then cooled to ambient temperature precipitating a solid. The solid was collected by filtration and rinsed with diethyl ether to yield 44.5 mg (64%) of a metallic blue solid, m.p. 205-207 °C: ^{1}H NMR [500 MHz, CD_2Cl_2] δ 7.89 (d, 1 H, J = 14.5 Hz), 7.75 (s, 2 H), 7.68 (d, 2 H, J = 3.5 Hz), 7.40 (s, 2 H), 7.26 (t, 2 H, J = 4.5 Hz), 7.09 (d, 1 H, J = 14.5 Hz), 3.52 (t, 4 H, J = 5.0 Hz), 2.81 (t, 4 H, J = 6.0 Hz), 2.05 (t, 4 H, J = 7.0 Hz); λ_{max} (CH_2Cl_2) 820 nm (ε = 3.90 × 10^4 M^{-1}cm^{-1}), 718 nm ε = 2.90 × 10^4 M^{-1}cm^{-1}). HRMS (ESI) *m/z* 506.0517 (calcd for $C_{27}H_{24}NS_2{}^{80}Se$: 506.0510).

ChPIR-846$_3$

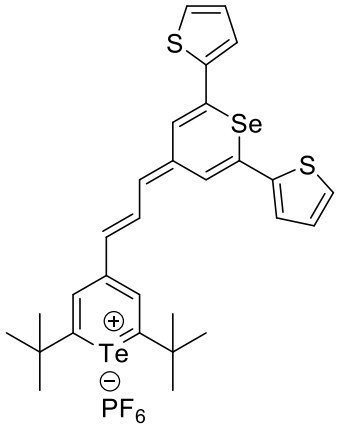

(*E*)-2,6-di-*tert*-butyl-4-(3-(2,6-di(thien-2-yl)-4H-selenopyran-4-ylidene)prop-1-en-1-yl)telluropyrylium hexafluorophosphate

2,6-di-*tert*-butyl-4-methyltelluropyrylium hexafluorophosphate[3] (44.1 mg, 0.095 mmol) and 2-(2,6-di(thien-2-yl)-4H-selenopyran-4-ylidene)acetaldehyde[1] (36.3 mg, 0.104 mmol) were dissolved in acetic anhydride (2.00 mL) and heated at 105 °C for 90 s in a test tube. The reaction mixture was then cooled to ambient temperature. Acetonitrile (1.0 mL) and diethyl ether (3.0 mL) were added precipitating a solid. The solid was collected by filtration and rinsed with diethyl ether to yield 16.0 mg (28%) of a metallic red solid, m.p. 211-213 °C: ^{1}H NMR [500 MHz, CD_2Cl_2] δ 8.59 (t, 1 H, J = 13.5 Hz), 7.85 (s, 2 H), 7.65 (d, 2 H, J = 5.0 Hz), 7.55 (s, 2 H), 7.23 (t, 2 H, J = 4.5 Hz), 6.79 (d, 1 H, J = 13.5 Hz), 6.62 (d, 1 H, J = 13.5 Hz), 1.53 (s, 18 H); λ_{max} (CH_2Cl_2) 846 nm (ε = 1.2 × 10^5 M^{-1}cm^{-1}). HRMS (ESI) *m/z* 653.0085 (calcd for $C_{29}H_{31}S_2{}^{80}Se^{130}Te$: 653.0089).

CHPIR-846$_6$

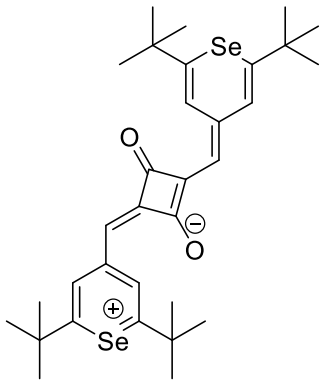

(*E*)-2-((2,6-di-*tert*-butyl-4H-selenopyran-4-ylidene)methyl)-4-((2,6-di-*tert*-butylselenopyrylium-4-yl)methylene)-3-oxocyclobut-1-en-1-olate[4]

Synthetic procedure can be found in reference 4. Experimental data are in agreement with the literature.

ChPIR-904

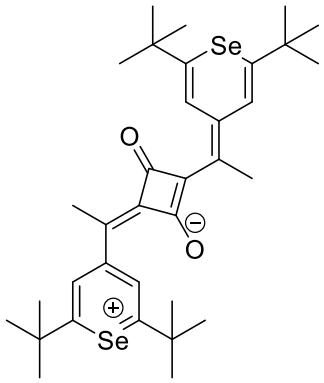

(*E*)-2-(1-(2,6-di-*tert*-butyl-4H-selenopyran-4-ylidene)ethyl)-4-(1-(2,6-di-*tert*-butylselenopyrylium-4-yl)ethylidene)-3-oxocyclobut-1-en-1-olate

Synthetic procedure can be found in reference 4. Experimental data are in agreement with the literature.

ChPIR-814

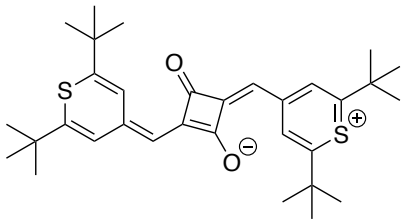

(*Z*)-2-((2,6-di-*tert*-butyl-4H-thiopyran-4-ylidene)methyl)-4-((2,6-di-*tert*-butylthiopyrylium-4-yl)methylene)-3-oxocyclobut-1-en-1-olate

Synthetic procedure can be found in reference 4. Experimental data is in agreeance with the literature.

ChPIR-868

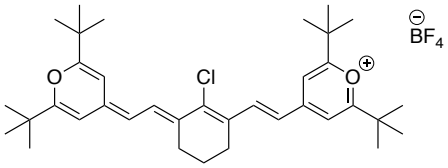

2,6-di-*tert*-butyl-4-((*E*)-2-((*E*)-2-chloro-3-(2-(2,6-di-*tert*-butyl-4H-pyran-4-ylidene)ethylidene)cyclohex-1-en-1-yl)vinyl)pyrylium trifluoromethanesulfonate[5]

Synthetic procedure can be found in reference 5. Experimental data is in agreeance with the literature.

Synthesis of precursors:

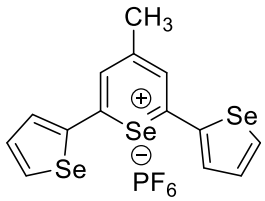

4-methyl-2,6-di(selenophen-2-yl)selenopyrylium hexafluorophosphate

2,6-di(selenophen-2-yl)-4*H*-selenopyran-4-one (0.120 g, 0.288 mmol) was dissolved in anhydrous THF (3.85 mL) in a flame-dried flask under nitrogen. A solution of 3.0 M MeMgBr (0.29 mL, 0.86 mmol) was added dropwise to the flask, and the mixture was allowed to stir for 1.5 h. The reaction mixture was then poured into a 10% aqueous HPF_6 solution (30 mL). The product was extracted with CH_2Cl_2 (3 × 25 mL) and the combined organic extracts were dried over Na_2SO_4 and concentrated under reduced pressure. The crude product was recrystallized from CH_3CN/ether to yield 95.2 mg (59%) of a bright red solid, mp >260 ˚C: ^{1}H NMR [500 MHz, CD_3CN] δ 8.82 (d, 2 H, *J* = 6.0 Hz), 8.19 (d, 2 H, *J* = 4.0 Hz), 8.12 (s, 2 H), 7.62-7.59 (m, 2 H), 2.69 (s, 3 H); ^{13}C NMR [75.5 Hz, CD_3CN] δ 170.4, 167.5, 145.3, 144.6, 136.8, 134.1, 132.6, 27.2; HRMS (ESI) *m/z* 418.8341 (calcd for $C_{14}H_{11}{}^{80}Se_3^+$: 418.8351).

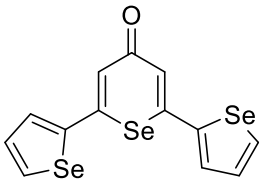

2,6-di(selenophen-2-yl)-4*H*-selenopyran-4-one

2,6-Di(selenophen-2-yl)tetrahydro-4*H*-selenopyran-4-one (0.730 g, 1.73 mmol) was dissolved in anhydrous toluene (15.0 mL) and added to a flame-dried flask under argon. 2,3-Dichloro-5,6-dicyano-1,4-benzoquinone (DDQ) (0.983 g, 4.33 mmol) and methane sulfonic acid (1 drop) were added in one portion. The reaction mixture was refluxed for 1.5 h and then cooled to ambient temperature. The reaction mixture was diluted with CH_2Cl_2 (50 mL) and washed with saturated aqueous $NaHCO_3$ (50 mL). The organic layer was separated, dried over $MgSO_4$, and concentrated under reduced pressure. The crude product was purified on SiO_2 eluting with 20% EtOAc/CH_2Cl_2 (R_f 0.47). The product was recrystallized from CH_2Cl_2/hexanes to yield 0.505 g (70%) of a yellow crystalline solid, m.p. 138-139 ˚C: ^{1}H NMR [500 MHz, $CDCl_3$] δ 8.19 (d, 2 H, *J* = 5.5 Hz), 7.62 (d, 2 H, *J* = 3.5 Hz), 7.38 (t, 2 H, *J* = 5 Hz, 7.15 (s, 1 H, *J* = 5 Hz); ^{13}C NMR [75.5 Hz, $CDCl_3$] δ 184.2, 147.4, 145.4, 134.7, 130.8, 129.6, 126.7.

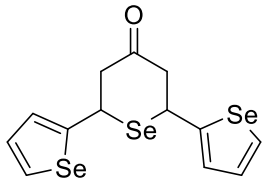

2,6-di(selenophen-2-yl)tetrahydro-4*H*-selenopyran-4-one

Selenium powder (0.314 g, 3.98 mmol), $NaBH_4$ (0.301 g, 7.95 mmol), H_2O (4.50 mL), *i*-PrOH (9.00 mL) and K_2HPO_4 (0.908 g, 3.98 mmol) were added to a flask that had been flushed with nitrogen for 15 min. The resulting mixture was stirred for 0.5 h. (1*E*,4*E*)-1,5-Di(selenophen-2-yl)penta-1,4-dien-3-one[2] (0.900 g, 2.65 mmol) dissolved in THF (4.50 mL) was added in one portion. The resulting mixture was stirred for 3 h and was subsequently diluted with H_2O (50 mL) and extracted with CH_2Cl_2 (3 × 30 mL). The combined organic extracts were dried over $MgSO_4$ and concentrated in vacuo. The crude product was purified on SiO_2 eluting with CH_2Cl_2 (R_f = 0.65) to yield 0.727 g (65%) of a yellow oil. ^{1}H NMR [500 MHz, $CDCl_3$] δ 7.96-7.94 (m , 2 H), 7.17-7.12 (m 4 H), 4.96 (dd, 1 H, *J* = 3.0, 12.5 Hz), 4.92 (t, 1 H, *J* = 6.5 Hz), 3.27-3.23 (m, 2 H), 3.18 (t, 1 H, *J* = 13.0 Hz); ^{13}C NMR [75.5 Hz, $CDCl_3$] δ 207.0, 206.7, 152.6, 150.6, 130.9, 130.7, 129.4, 129.2, 127.6, 126.9, 52.5, 50.9, 28.3, 36.2.

ChPIR-779

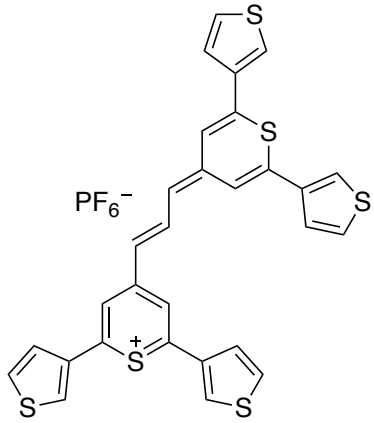

(*E*)-4-(3-(2,6-di(thien-3-yl)-4*H*-thiopyran-4-ylidene)prop-1-en-1-yl)-2,6-di(thiophene-3-yl)thiopyrylium hexafluorophosphate

4-Methyl-2,6-di(thiophene-3-yl)thiopyrylium hexafluorophosphate (50.0 mg, 0.119 mmol) and 2-(2,6-di(thiene-3-yl)-4H-thiopyran-4-ylidene)acetaldehyde (40 mg, 0.132 mmol) were dissolved in acetic anhydride (2.00 mL). The resulting mixture was heated at 105 °C for 15 min and was then cooled to ambient temperature precipitating a crystalline product. The product was collected by filtration and rinsed with diethyl ether to yield 77.6 mg (93 %) of a dark green solid, mp > 260 °C: ^{1}H NMR [500 MHz, CD_2Cl_2] δ 8.83 (m, 1 H), 8.71 (s, 1 H), 8.33 (m, 2 H), 8.19 (m, 2 H), 7.98 (m, 1 H), 7.89 (s, 1 H), 7.56 (m, 5 H), 7.38 (m, 5 H), 6.63 (d, 1 H, *J* = 13.0 Hz); λ_{max} (CH_2Cl_2) 779 nm (ε= 2.3 × 10^5 M^{-1} cm^{-1}), 698 nm (ε= 4.6 ×10^4 M^{-1} cm^{-1}), 428 nm (ε= 2.0 ×10^4 M^{-1} cm^{-1}); HRMS (ESI) m/z 558.9803 (calcd for $C_{29}H_{19}S_6$: 558.9806).

Novel precursors to ChPIR-779

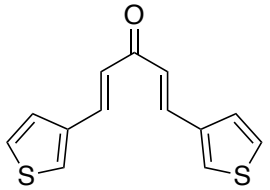

(1*E*,4*E*)-1,5-di(thien-3-yl)penta-1,4-dien-3-one

Thiophene-3-carbaldehyde (5.00 g, 44.6 mmol) and acetone (1.29 g, 22.3 mmol) were dissolved in EtOH (40 mL) and KOH (1.25 g, 22.3 mmol) dissolved in H_2O was added slowly. The resulting mixture was stirred for 3 h at ambient temperature and was then diluted with H_2O (100 mL). The products were extracted with CH_2Cl_2 (3 × 50 mL) and the combined organic extracts were dried over $MgSO_4$ and concentrated *in vacuo*. The crude product was recrystallized from CH_2Cl_2/hexanes to yield 3.63 g (66%) of a bright yellow, crystalline solid, mp 137-138 °C: ^{1}H NMR [400 MHz, $CDCl_3$] δ 7.71 (d, 2 H, *J* = 16.0 Hz), 7.57 (s, 2 H), 7.37 (s, 4 H), 6.87 (d, 2 H, *J* = 16.0 Hz); ^{13}C NMR [100 MHz, $CDCl_3$] δ 189.3, 138.1, 136.5, 128.8, 127.0, 125.2, 125.2; HRMS (ESI) *m/z* 247.0244 (calcd for $C_{13}H_{11}OS_2$: 247.0246).

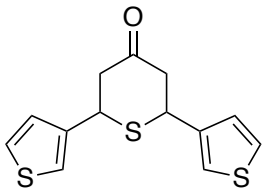

2,6-di(thien-3-yl)tetrahydro-4*H*-thiopyran-4-one

(1*E*,4*E*)-1,5-Di(thiophen-3-yl)penta-1,4-dien-3-one (2.00 g, 8.11 mmol) was dissolved in THF (12 mL). To this mixture *i*-PrOH (24 mL) and K_2HPO_4 (2.22 g, 9.74 mmol) dissolved in H_2O (12 mL) were added followed by the addition of NaHS (0.823 g, 8.94 mmol). The resulting mixture was stirred overnight at ambient temperature and was then diluted with H_2O (100 mL). The products were extracted with CH_2Cl_2 (3 × 50 mL). The combined organic extracts were dried over $MgSO_4$ and concentrated *in vacuo*. The crude product was purified on SiO_2 eluted with CH_2Cl_2 (R_f = 0.65) to yield 2.17 g (95%) of a light-yellow solid, mp 50-55 °C: ^{1}H NMR [400 MHz, $CDCl_3$] δ 7.31 (m, 2 H), 7.22-7.09 (m, 4 H), 4.46 (dd, 1 H, *J* = 3.4, 11.8 Hz), 4.33 (m, 1 H), 3.04 (m, 4 H); ^{13}C NMR [100 MHz, $CDCl_3$] δ 207.9, 207.2, 140.9, 139.9, 127.3, 126.5, 126.4, 126.4, 122.1, 121.8, 50.34, 43.27, 40.16; HRMS (ESI) *m/z* 302.9942 (calcd for $C_{13}H_{12}NaOS_3$: 302.9943).

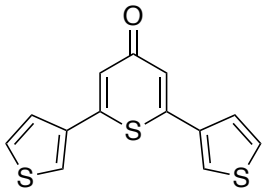

2,6-di(thien-3-yl)-4*H*-thiopyran-4-one

2,6-Di(thien-3-yl)tetrahydro-4*H*-thiopyran-4-one (1.50 g, 5.35 mmol) was dissolved in anhydrous toluene (46.8 mL) and placed in a flame-dried flask under nitrogen. 2,3-Dichloro-5,6-dicyano-1,4-benzoquinone (DDQ, 3.04 g, 13.4 mmol) and $MeSO_3H$ (2 drops) were subsequently added. The resulting reaction mixture was heated at reflux for 1.5 h and then cooled to ambient temperature and diluted with saturated aqueous $NaHCO_3$ (50 mL). The product was extracted with CH_2Cl_2 (3 × 50 mL). The combined organic extracts were washed with brine, dried over $MgSO_4$, and concentrated *in vacuo*. The crude product was purified by column chromatography on SiO_2 eluted with 20% EtOAc/CH_2Cl_2 (R_f = 0.70), and recrystallized from CH_2Cl_2/hexanes to yield 1.09 g (73%) of a brown solid, mp 130-134 °C: ^{1}H NMR [400 MHz, $CDCl_3$] δ 7.69 (d, 2 H, *J* = 1.2 Hz), 7.45 (m, 2 H), 7.36 (d, 2 H, *J* = 4.8 Hz), 7.16 (s, 2 H); ^{13}C NMR [100 MHz, $CDCl_3$] δ 182.6, 146.5, 136.9, 127.8, 125.6, 125.2, 124.7; HRMS (ESI) *m/z* 276.9809 (calcd for $C_{13}H_9OS_3$: 276.9810).

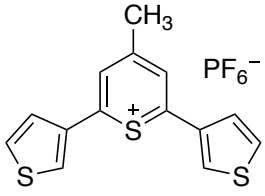

4-methyl-2,6-di(thien-3-yl)thiopyrylium hexafluorophosphate

In a flame-dried flask under nitrogen, 2,6-di(thien-3-yl)-4*H*-thiopyran-4-one (1.00 g, 3.62 mmol) was dissolved in anhydrous THF (24.2 mL). A solution of 3.0 M MeMgBr (1.30 g, 10.9 mmol) was added dropwise and the resulting solution was stirred at ambient temperature for 2 h. The reaction mixture was poured into 10% aqueous HPF_6 (60 mL). The products were extracted with a 9:1 mixture of CH_2Cl_2 and CH_3CN (3 × 50 mL). The combined organic layers were dried over $NaSO_4$ and concentrated *in vacuo*. The crude product was recrystallized from CH_3CN/ether to yield 506 mg (33%) of a brown solid, mp 163-167 °C: ^{1}H NMR [500 MHz, CD_3CN] δ 8.54 (s, 2 H), 8.45 (d, 2 H, *J* = 1.5 Hz), 7.79 (m, 2 H), 7.76 (d, 2 H, *J* = 5.0 Hz), 2.84 (s, 3 H); ^{13}C NMR [100 Mhz, $CDCl_3$] δ 164.7, 138.9, 131.7, 131.5, 130.5, 125.5, 109.5, 25.07; HRMS (ESI) *m/z* 275.0017 (calcd for $C_{14}H_{11}S_3$: 275.0017).

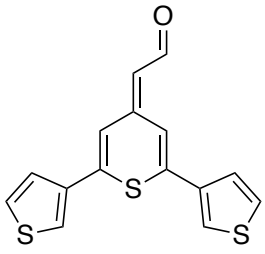

2-(2,6-di(thien-3-yl)-4*H*-thiopyran-4-ylidene)acetaldehyde

4-Methyl-2,6-di(thiophen-3-yl)thiopyrylium hexafluorophosphate (0.250 g, 0.595 mmol), *N,N*-dimethylthioformamide (DMF, 0.152 mL, 1.78 mmol), and acetic anhydride (2.50 mL) were combined in a round bottom flask and heated at 95 °C for 1.5 h. After the reaction mixture was cooled to ambient temperature, CH_3CN (2.0 mL) was added followed by the addition of ether. Chilling the resulting mixture overnight at -20 °C precipitated the iminium salt, which was isolated by filtration to yield a brown solid. The solid was hydrolyzed with saturated aqueous NaHCO3 (8.0 mL) in CH_3CN (8.0 mL) heated at reflux for 0.5 h. The solution was cooled to ambient temperature and diluted with H_2O (20 mL). The product was extracted with CH_2Cl_2 (3 × 35 mL). The combined organic extracts were dried over $MgSO_4$ and concentrated *in vacuo.* The crude product was purified on SiO_2 eluted with 10% EtOAc/CH_2Cl_2 eluent (R_f = 0.50), and recrystallized from CH_2Cl_2/hexanes to yield 0.059 g (33%) of a dark green/brown solid, mp 104-108 °C: ^{1}H NMR [400 MHz, CD_2Cl_2] δ 9.95 (d, 1 H, *J* = 6.0 Hz), 8.27 (s, 1 H), 7.67 (d, 2 H, *J* = 16.0 Hz), 7.42 (m, 4 H), 6.95 (s, 1 H), 5.68 (d, 1 H, *J* = 6.0 Hz) ; ^{13}C NMR [100 MHz, CD_2Cl_2] δ 187.8, 127.3, 125.1, 124.8, 123.9, 123.6, 122.9, 117.9, 117.1; HRMS (ESI) *m/z* 302.9967 (calcd for $C_{15}H_{11}OS_3$: 302.9967).

ChPIR-820$_3$

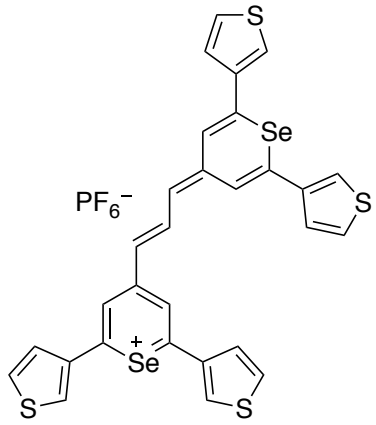

(E)-4-(3-(2,6-di(thien-3-yl)-4*H*-selenopyran-4-ylidene)prop-1-en-yl)-2,6-di(thiophene-3-yl)selenopyrylium hexafluorophosphate

4-Methyl-2,6-di(thien-3-yl)selenopyrylium hexafluorophosphate (50.0 mg, 0.107 mmol) and 2-(2,6-di(thien-3-yl)-4*H*-selenopyran-4-ylidene)acetaldehyde (40.0 mg, 0.114 mmol) in acetic anhydride (1.76 mL) were heated at 105 °C for 15 min. The reaction mixture was cooled to ambient temperature precipitating a crystalline solid. The solid was collected by filtered and rinsed with diethyl ether to yield 74.6 mg (87 %) of a dark green/brown solid, mp > 260 °C: ^{1}H NMR [500 MHz, CD_2Cl_2] δ 8.77 (m, 1 H), 8.49 (m, 1 H), 8.35 (s, 1 H), 8.11 (s, 1 H), 7.98 (m, 2 H), 7.71 (d, 1 H, J = 12.5 Hz), 7.38 (m, 11 H), 6.79 (d, 1 H, J = 12.5 Hz); λ_{max} (CH_2Cl_2) 807 nm (ε = 1.6 ×10^5 M^{-1} cm^{-1}), 453 nm (ε = 1.3 × 10^4 M^{-1} cm^{-1}). HRMS (ESI) *m/z* 654.8713 (calcd for $C_{29}H_{19}S_4{}^{80}Se_2$: 654.8695).

Novel precursors to ChPIR-820$_3$

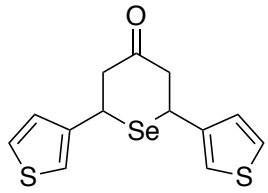

2,6-di(thien-3-yl)tetrahydro-4*H*-selenopyran-4-one

Selenium powder (0.962 g, 12.2 mmol), $NaBH_4$ (0.922 g, 24.4 mmol), K_2HPO_4 (2.78 g, 12.2 mmol), H_2O (14 mL), and *i*-PrOH (28 mL) were combined in a flask that had been flushed with nitrogen and stirred until Na_2Se formed. (1*E*,4*E*)-1,5-Di(thiophen-3-yl)penta-1,4-dien-3-one (2.00 g, 8.12 mmol) was dissolved in THF (14 mL) and added slowly to the other reagents. The resulting mixture was stirred at ambient temperature for 2 h and was then diluted with H_2O (100 mL). Products were extracted with CH_2Cl_2 (4 × 25 mL). The combined organic extracts were dried over $MgSO_4$ and concentrated *in vacuo*. The crude product was purified on SiO_2 eluted with CH_2Cl_2 (R_f = 0.70) to yield 2.80 g (95 %) of a yellow/orange product, mp 99-107 °C: ^{1}H NMR [400 MHz, $CDCl_3$] δ 7.30 (m, 2 H), 7.18 (d, 1 H, J = 1.6 Hz), 7.09 (m, 3 H), 4.70 (dd, 1 H, J = 3.8, 11.4 Hz), 4.56 (m, 1 H), 3.19 (m, 4 H); ^{13}C NMR [100 MHz, $CDCl_3$] δ 208.2, 141.9, 140.9, 127.5, 126.6, 126.3, 121.4, 121.1, 50.39, 49.43, 35.69, 33.28; HRMS (ESI) *m/z* 350.9388 (calcd for $C_{13}H_{12}NaOS_2{}^{80}Se$: 350.9387).

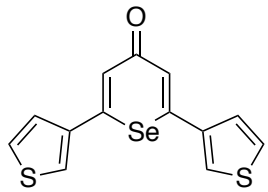

2,6-di(thien-3-yl)-4*H*-selenopyran-4-one

2,6-Di(thien-3-yl)tetrahydro-4*H*-selenopyran-4-one (2.00 g, 6.11 mmol) was dissolved in anhydrous toluene (53.5 mL) and placed in a flame-dried flask under nitrogen. DDQ (3.47 g, 15.3 mmol) and $MeSO_3H$ (2 drops) were subsequently added and the resulting mixture was heated at reflux for 1.5 h and then cooled to ambient temperature and diluted with saturated aqueous $NaHCO_3$ (50 mL). The product was extracted with CH_2Cl_2 (3 × 35 mL). The combined organic extracts were washed with brine, dried over $MgSO_4$, and concentrated *in vacuo*. The crude product was purified by column chromatography on SiO_2 eluted with a 20% EtOAc/CH_2Cl_2 (R_f = 0.50), and recrystallized from CH_2Cl_2/hexanes to yield 0.96 g (49%) of a brown crystalline solid, mp 150-156 °C: ^{1}H NMR [400 MHz, $CDCl_3$] δ 7.66 (t, 2 H, J = 1.5 Hz), 7.48 (t, 3 H, J = 2.8, 4.4 Hz), 7.36 (d, 3 H, J = 4.8 Hz); ^{13}C NMR [100 MHz, $CDCl_3$] δ 184.7, 147.9, 138.8, 127.8, 126.8, 125.2, 124.6; HRMS (ESI) *m/z* 324.9256 (calcd for $C_{13}H_9OS_2{}^{80}Se$: 324.9255).

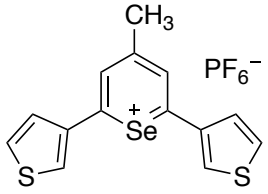

4-methyl-2,6-di(thien-3-yl)selenopyrylium hexafluorophosphate

In a flame-dried flask under nitrogen, 2,6-di(thien-3-yl)-4*H*-selenopyran-4-one (0.959 g, 2.97 mmol) was dissolved in anhydrous THF (25.7 mL). A solution of 3.0 M MeMgBr (1.24 g, 10.4 mmol) was added dropwise and the resulting solution was stirred at ambient temperature for 2 h. The reaction mixture was poured into 10% aqueous HPF_6 (60 mL) and the products were extracted with a 9:1 mixture of CH_2Cl_2 and CH_3CN (3 × 50 mL). The combined organic extracts were dried over $NaSO_4$ and concentrated *in vacuo*. The crude product was recrystallized from CH_3CN/ether to yield 1.06 g (77%) of a pink/red solid, mp >260 °C: ^{1}H NMR [400 MHz, CD_3CN] δ 8.45 (s, 2 H), 8.41 (m, 2 H), 7.79 (m, 2 H), 7.71 (dd, 2 H, J = 1.4, 5.4 Hz), 2.75 (s, 3 H); ^{13}C NMR [100 MHz, $CDCl_3$] δ 166.9, 137.6, 131.8, 131.3, 130.7, 125.6, 110.0, 26.49; HRMS (ESI) *m/z* 322.9462 (calcd for $C_{14}H_{11}S_2{}^{80}Se$: 322.9462).

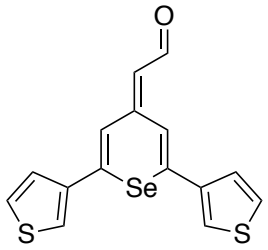

2-(2,6-di(thien-3-yl)-4*H*-selenopyran-4-ylidene)acetaldehyde

4-Methyl-2,6-di(thiophen-3-yl)selenopyrylium hexafluorophosphate (0.500 g, 1.07 mmol), DMF (0.286 g, 3.21 mmol), and acetic anhydride (5.0 mL) were combined in a round bottom flask and heated at 95 °C for 1.5 h. After the reaction mixture was cooled to ambient temperature, CH3CN (1.0 mL) was added followed by the addition of ether. Chilling the resulting mixture overnight at -20 °C precipitated the iminium salt, which was isolated by filtration to yield a brown solid. The solid was hydrolyzed with saturated aqueous NaHCO3 (16 mL) in CH3CN (16 mL) heated at reflux for 1.5 h. The reaction mixture was cooled to ambient temperature and diluted with H_2O (40 mL). The products were extracted with CH_2Cl_2 (4 × 35 mL). The combined organic extracts were dried over $MgSO_4$ and concentrated *in vacuo*. The crude product was purified on SiO_2 eluted with 10% EtOAc/CH_2Cl_2 eluent (R_f = 0.49), and recrystallized from CH_2Cl_2/hexanes to yield 0.157 g (42%) of a brown crystalline solid, mp 99-108 °C: ^{1}H NMR [500 MHz, $CDCl_3$] δ 10.1 (d, 1 H, J = 5.5 Hz), 8.37 (s, 1 H), 7.59 (s, 1 H), 7.54 (s, 1 H), 7.44 (s, 2 H), 7.39 (d, 1 H, J = 4.5 Hz), 7.33 (d, 1 H, J = 4.5 Hz), 6.99 (s, 1 H), 5.86 (d, 1 H, J = 6.0 Hz); ^{13}C NMR [100 MHz, $CDCl_3$] δ 188.7, 148.3, 139.8, 139.8, 139.5, 138.9, 127.4, 127.3, 125.2, 124.9, 124.6, 123.7, 123.4, 120.4, 119.5; HRMS (ESI) *m/z* 350.9413 (calcd for $C_{15}H_{11}OS_2{}^{80}Se$: 350.9411).

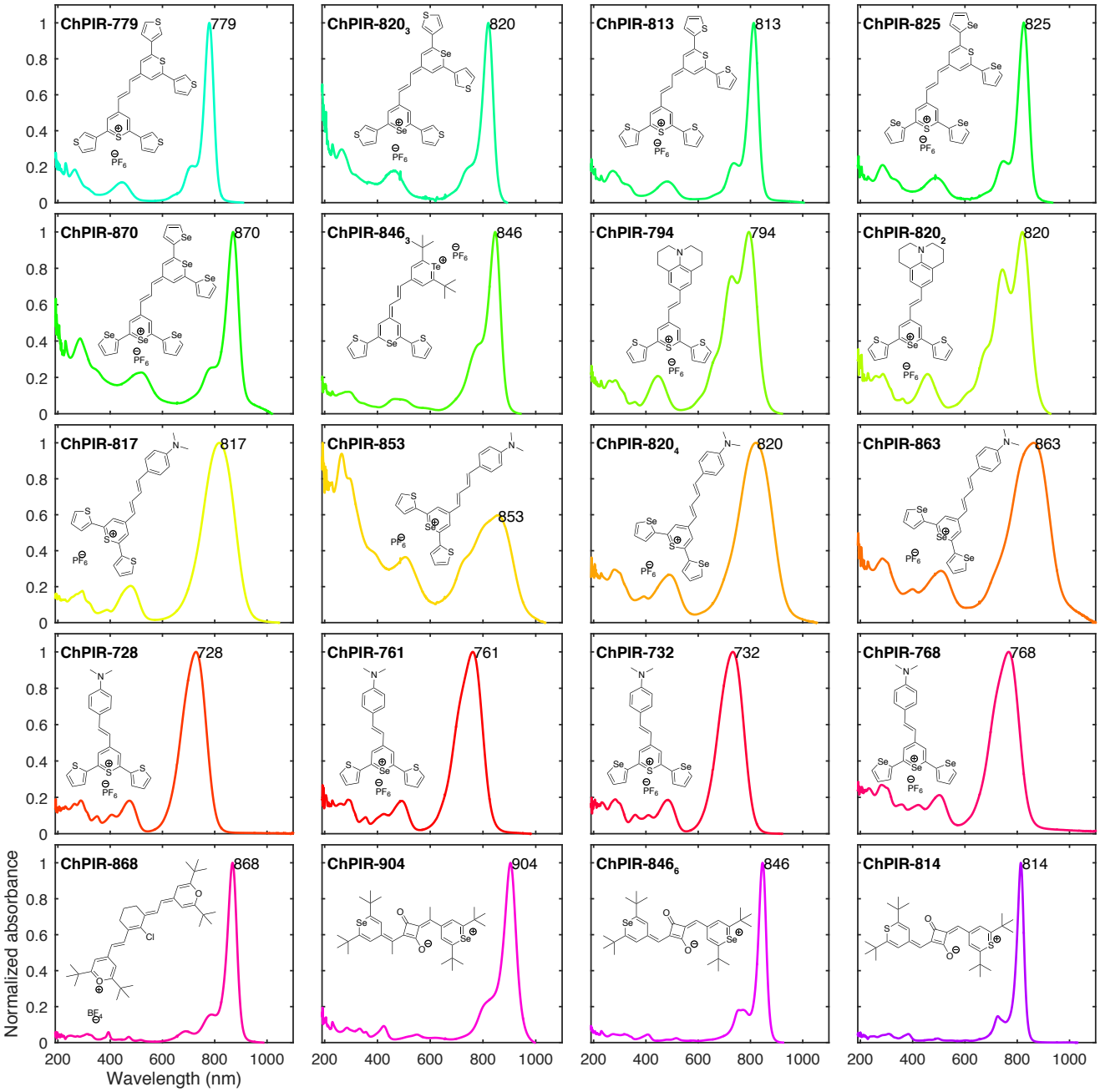

Figure S1. ChPIR dyes and their absorbance spectra in CH_2Cl_2.

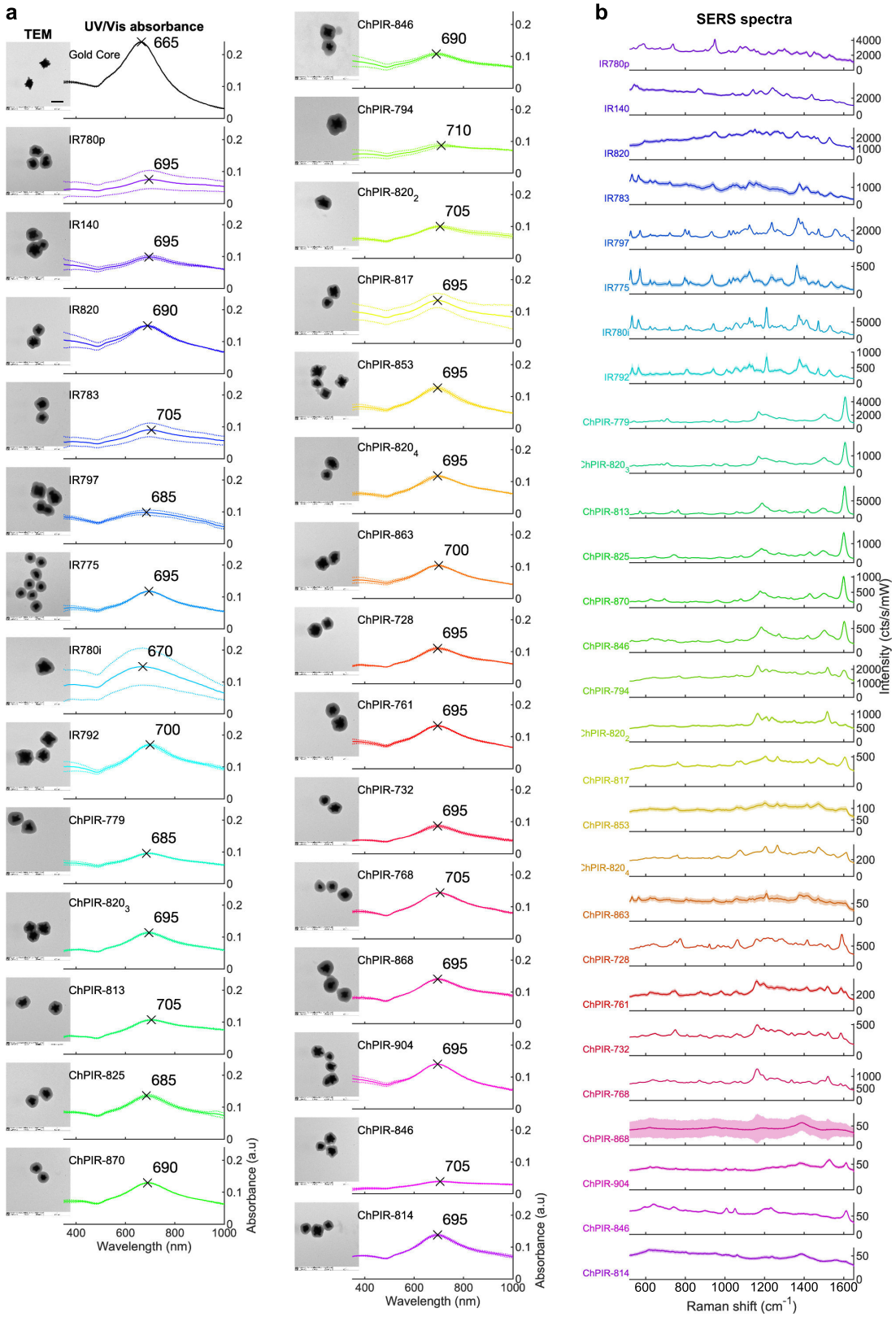

Fig. S2. SERRS nanoparticles synthesized using commercial IR and ChPIR dyes as reporters. (a) TEM images show the formation of a continuous silica shell around the gold nanostars core. Scale bars correspond to 100 nm. It is seen that absorbance is dominated by the plasmonic nanoparticle, not the IR dye. Solid lines indicate the mean absorbance from 3 independent silication reactions and dotted lines indicate standard deviations. High deviation indicates that the reaction is prone to aggregation. Low mean absorbance corresponds to low nanoprobe yield. (b) The Raman signature of each nanoparticle corresponds to the adsorbed reporter dye. Mean spectra (line) and standard deviations (shading) are shown for 98-point scans. High intensities are observed for dyes with absorbance near 785 nm, and low signals for dyes absorbing in higher wavelengths.

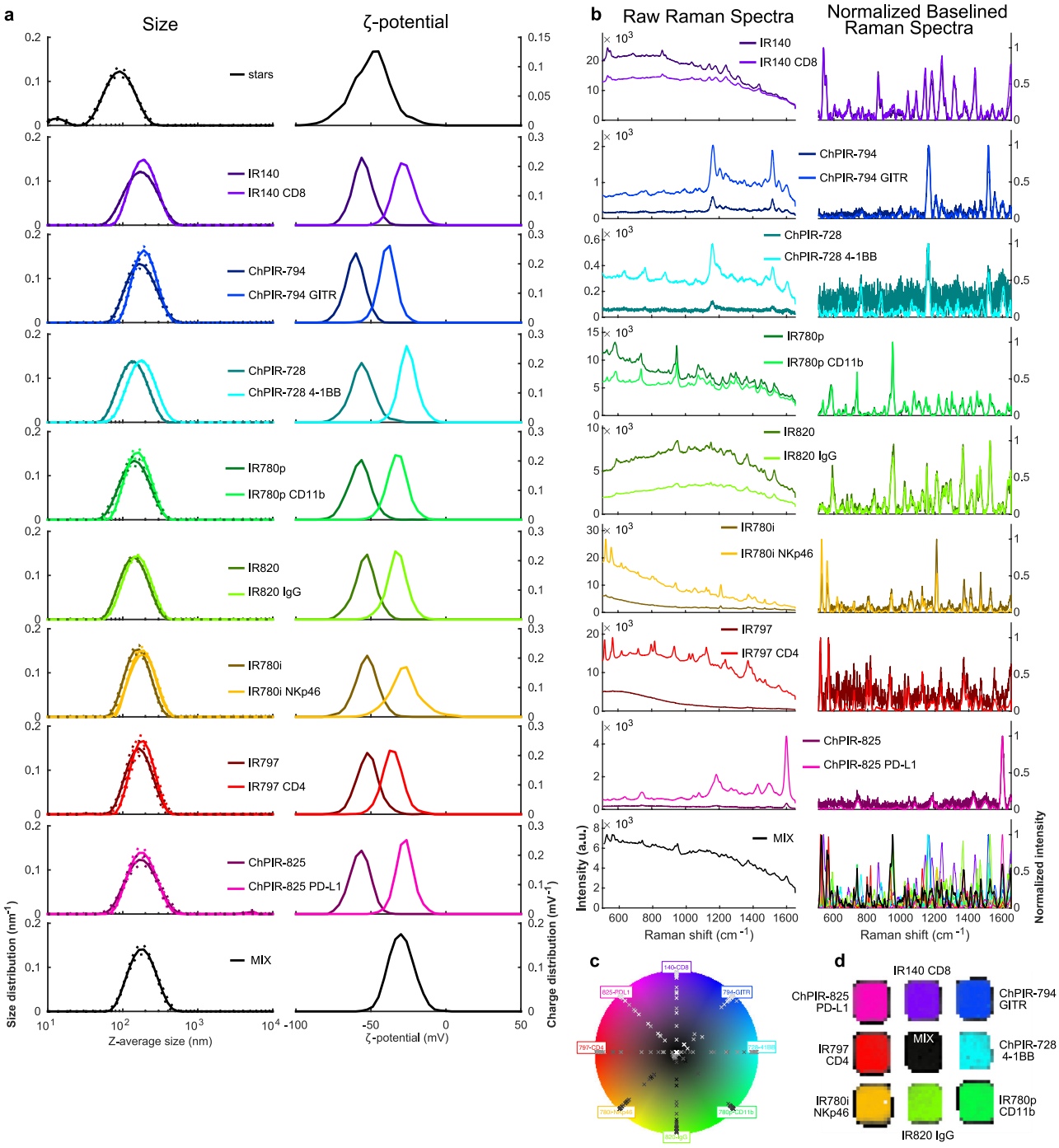

Fig. S3. (a) Physical characterization (size, left; ζ-potential, right) of SERRS nanoprobes at different stages of synthesis: solid lines represent mean and dotted lines standard deviation (n=3). Top row: gold nanostars prior to silication. Rows 2 to 9: 8 different flavors, each consisting of a distinct Raman reporter dye and a unique antibody. Row 10: mixture of the 8 flavors, as prepared for injections. (b) Raw spectra from nanoparticles before and after antibody conjugation. Intensity differences are due to different concentrations; the concentration of the nanoparticles was adjusted after conjugation, the mean intensity from point spectra is shown (n=98). After baseline correction and normalization, the spectra appear identical. The spectrum from the injected mix (black, bottom row) exhibits peaks from all constituent nanoparticles. (c) Colorspace projection of the 8 nanotags showing the colors assigned to individual spectra after nn-LS unmixing. Spectra from pure populations are projected closer to the circumference and assigned a saturated color. Spectra from the mixed sample are weighted equally by all basis vectors, and as such they are projected to the center. (d) Multiplexed image from a 1536-well plate, each pixel is colored based on the projection of its spectrum after nn-LS using the reference spectra above.

a

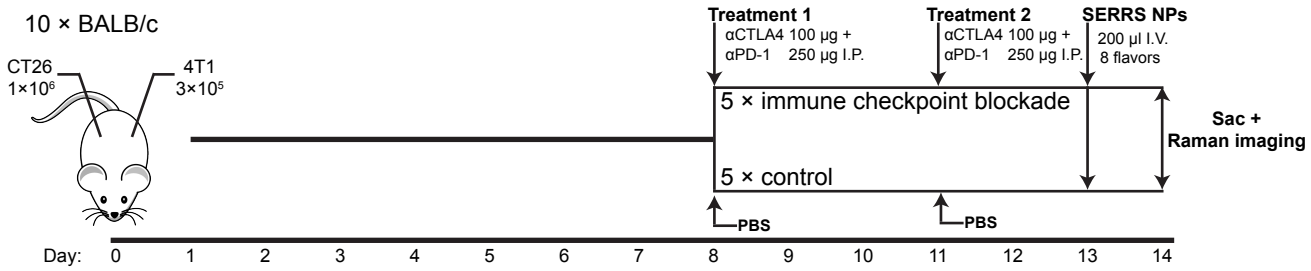

b

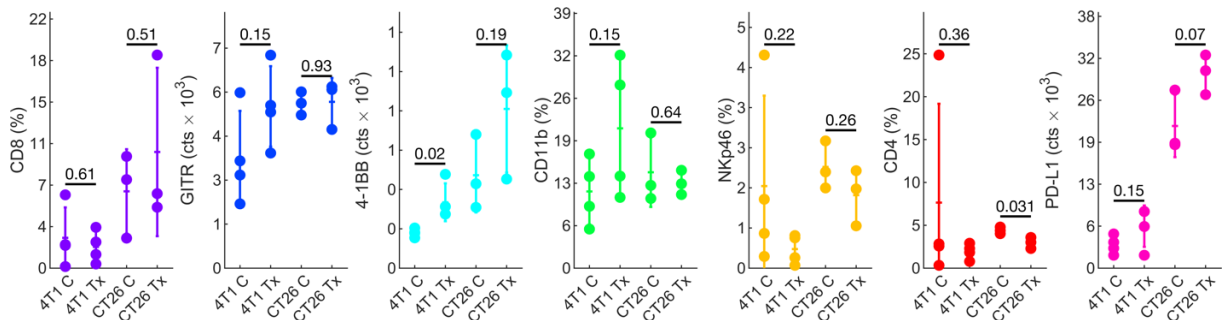

Fig. S4 Mouse model and treatment. (a) Bilateral subcutaneous flank syngeneic mouse model of immune checkpoint blockade for 8-plex imaging. (b) Flow cytometry analysis of the selected markers showed early, but not statistically significant, tumor treatment response.

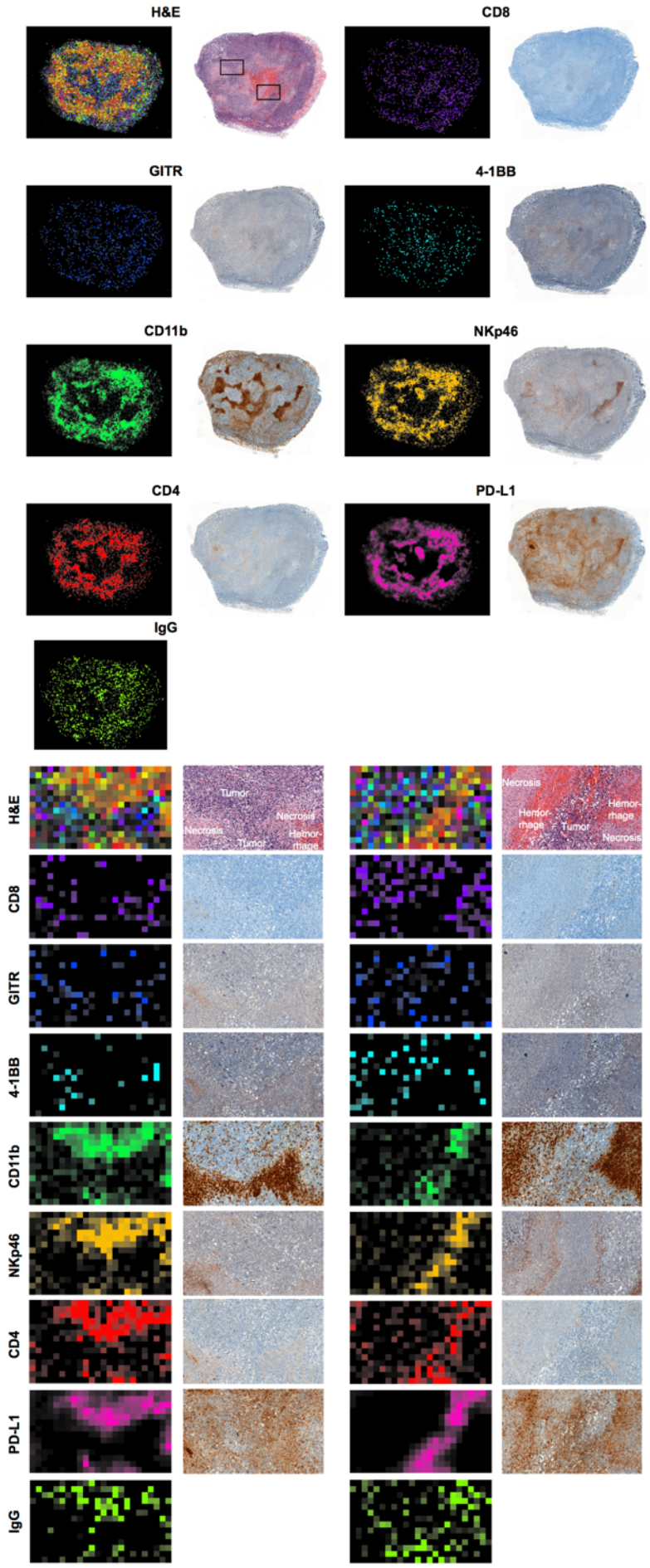

Fig. S5. Histological validation. Top: Full-tumor images show the distribution of each target as determined using Raman imaging and IHC. Raman images are derived from the same sample, split into channels, and mathematically assigned to pseudo color. IHC images were taken from different sections of the tumor, and exhibit variability of staining intensity dependent of antibody affinity and target abundance.
Bottom: Raman RadiCol images and histological images of the same areas, indicated by boxes on the the H&E image of the whole tumor (top left). The IHC images exhibit variable results as some antibodies provide non-uniform contrast: PD-L1, GITR show very high background; and CD11b demonstrates non-specific signal due to staining of necrotic regions. The Raman images provide high net signal from areas that were identified (via H&E stain) to contain viable tumor, and low net signal from areas of necrosis and hematoma. Within the viable tumor regions, the Raman images recapitulate the expression profile of the IHC images, i.e., high signals for CD11b, PD-L1, NKp46, and low signals for the remaining biomarkers.

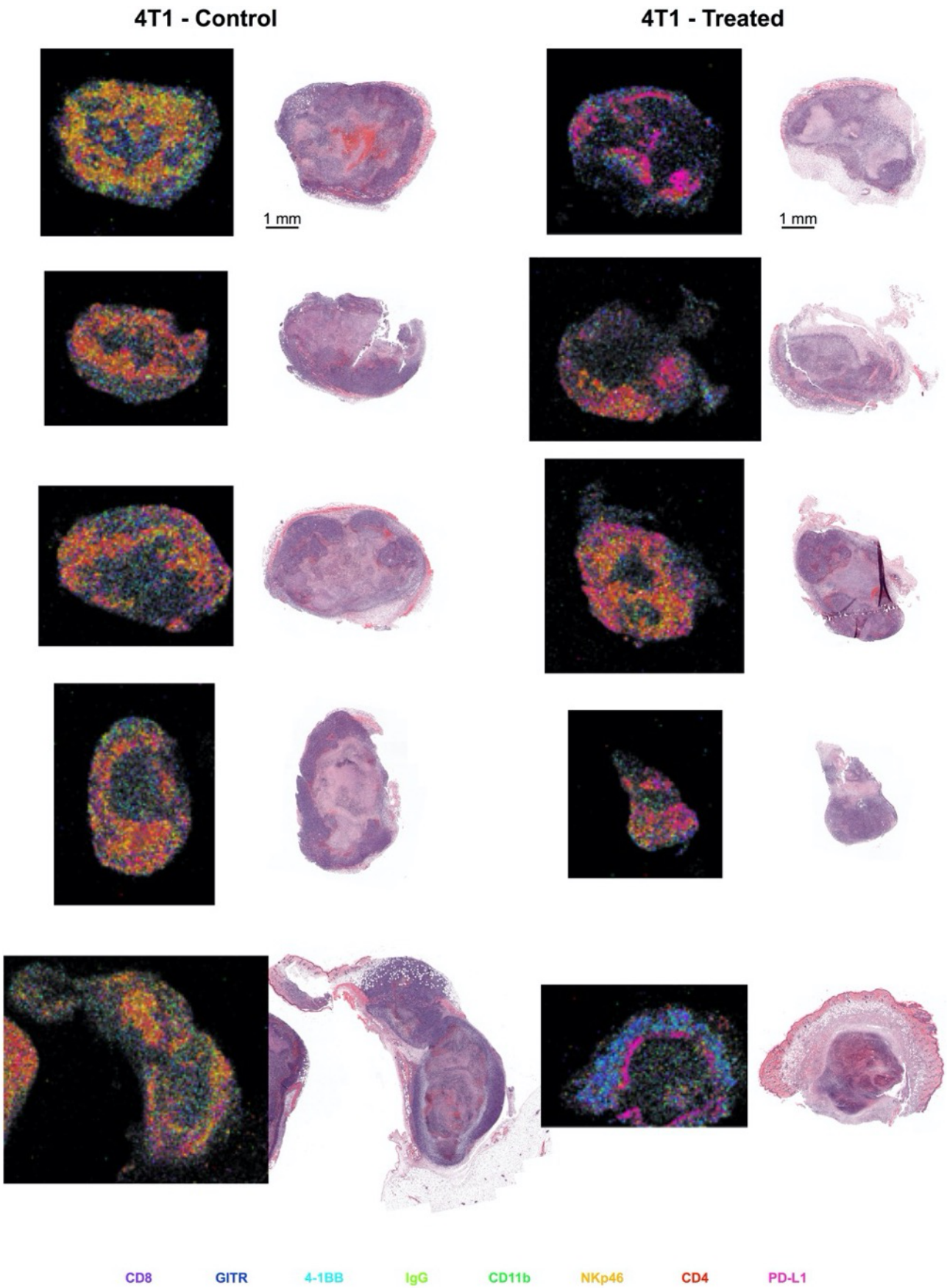

Fig. S6. RadiCol images vs. H&E for 4T1 tumors. Comparison of RadiCol Raman images and H&E stained sections for murine tumors from 4T1-tumor-bearing animals receiving immune checkpoint blockade (right) or sham treatment (left).

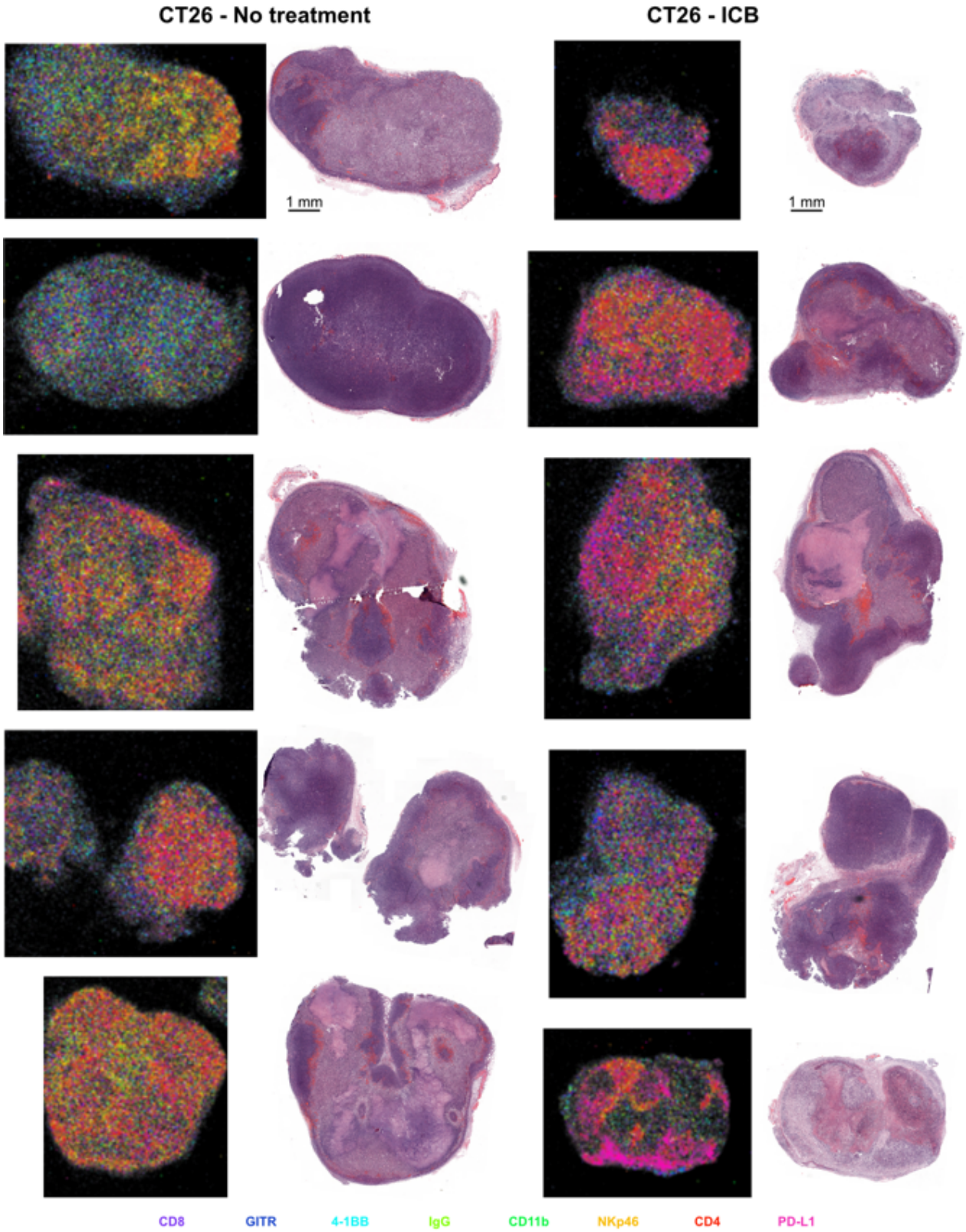

Fig. S7. RadiCol images vs. H&E for CT26 tumors. Comparison of RadiCol Raman images and H&E stained sections for murine tumors from CT26-tumor-bearing animals receiving immune checkpoint blockade (right) or sham treatment (left).

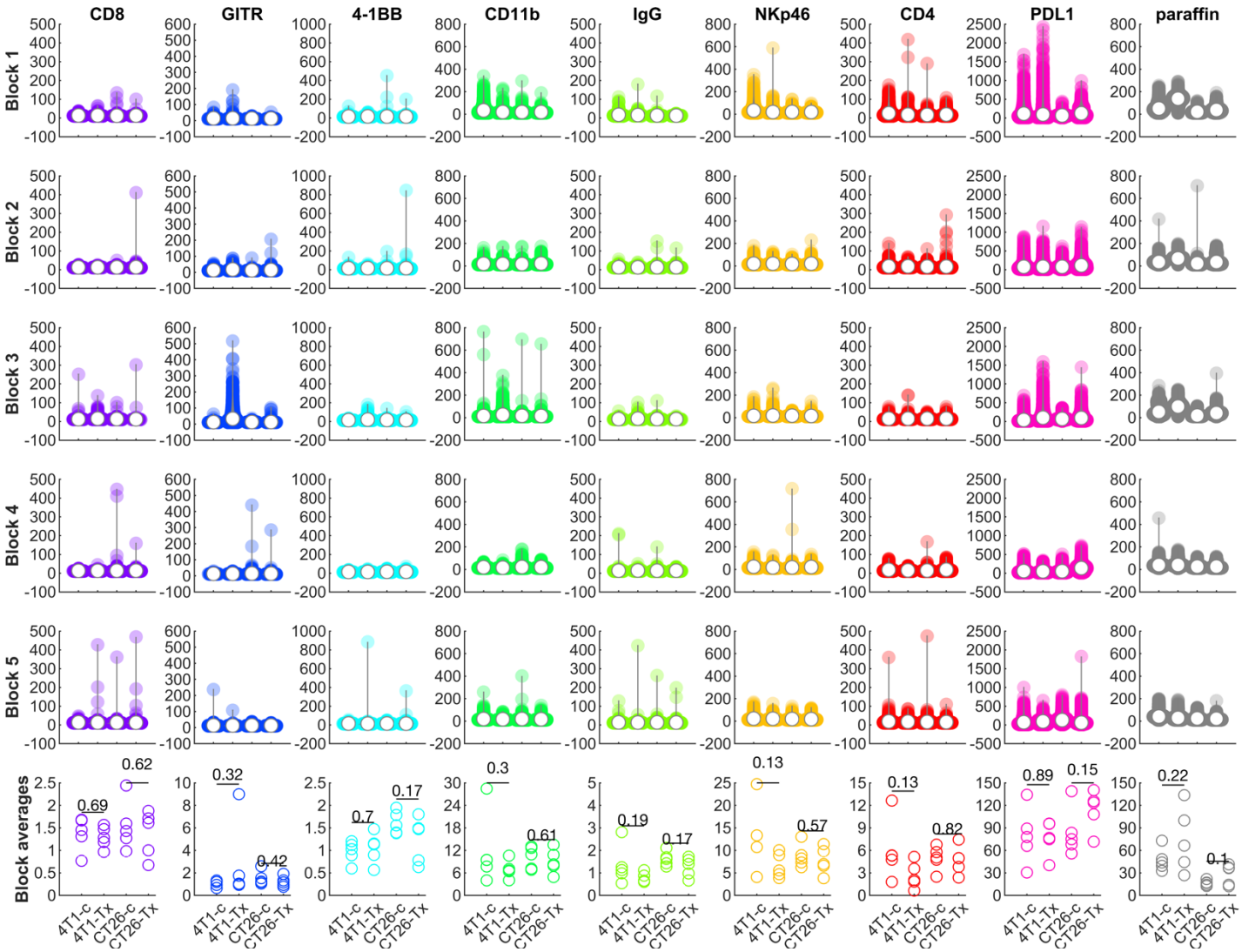

Fig. S8. Pixel wise score distributions of the 8 markers. Each row corresponds to a single paraffin block, containing four tumors from 2 mice (namely a 4T1 and a CT26 tumor from a mouse receiving ICB therapy, and a 4T1 and a CT26 tumor from a mouse receiving sham treatment). White circles show the mean score for each tumor. The plots appear in the order corresponding to the images from Figs. S6-S7. No statistically significant trends are evident with pixel-wise analysis of the individual markers.

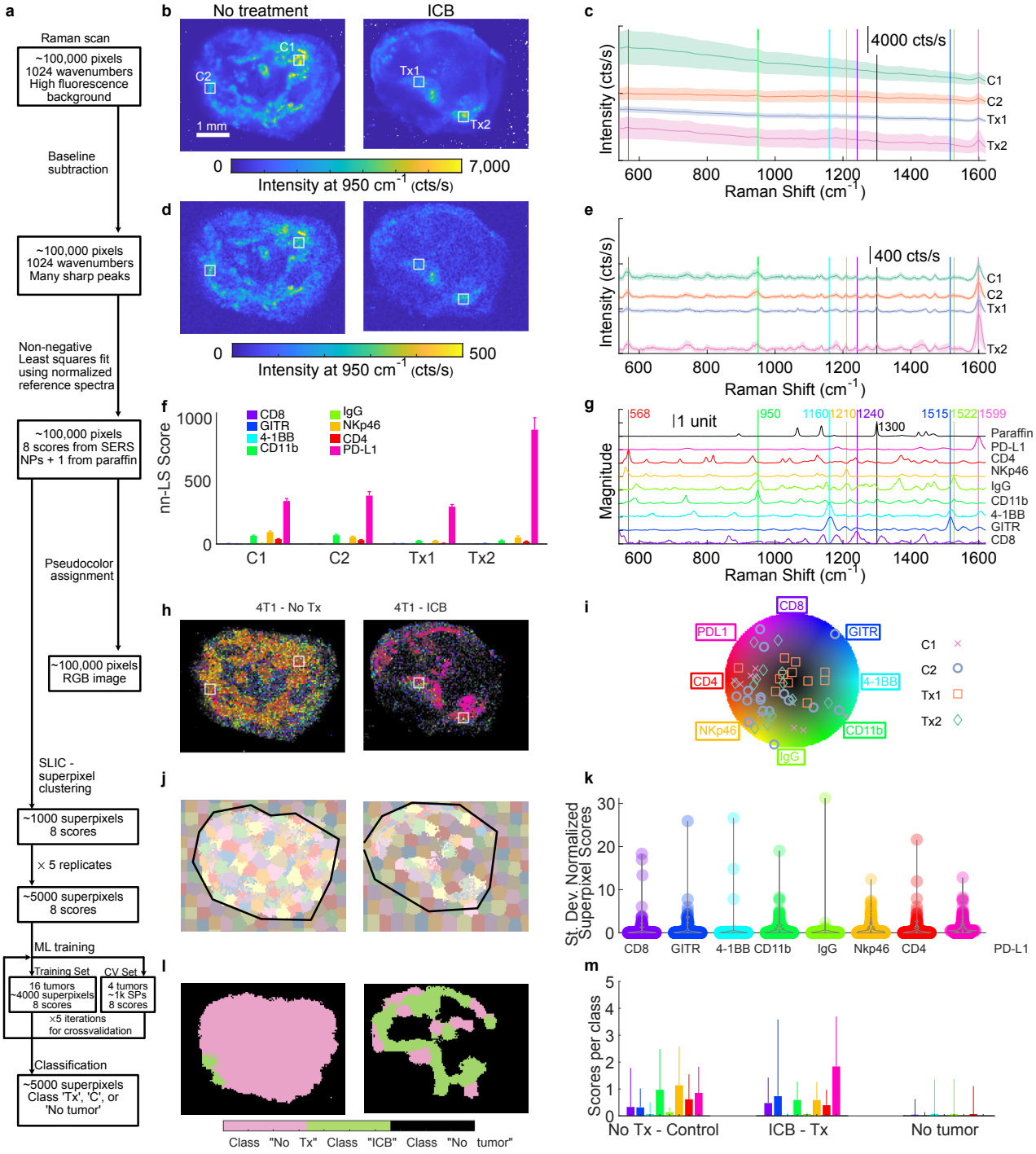

Figure *S9*. Spectral analysis leading to image segmentation and ML. (a) Data flow for multiplexed image visualization and ML model calibration. (b) A Raman image showing only one wavenumber provides little information. (c) Raw spectra acquired from indicated areas have a high fluorescence background. (d) Images produced after removal of fluorescence baseline. (e) Raman spectra from the same areas after baseline subtraction. (f) Quantitative marker profiles for the indicated areas obtained after nn-LS fit of the spectra in (e). (g) Reference spectra used for spectral unmixing via nn-LS. (h) Multiplexed molecular maps of the samples. (i) Projections of a small number of pixels from each of the 4 indicated areas are shown, indicating distinct distributions of markers for each sample. (j) Superpixel segmentation groups neighboring pixels with the same biomarker profile. Superpixel compactness is controlled by the parameter *a*. In this example $a=1\times 10^{-3}$ m^{-2} is too small yielding diffuse superpixels). (k) Mean superpixel scores on the 8 biomarkers. Each biomarker was normalized to unit variance. (l) SML model classifying the superpixels into No Treatment "No Tx", treatment "ICB", and "No tumor" areas. (m) Characteristic (mean) biomarker expression of superpixels assigned to each group.

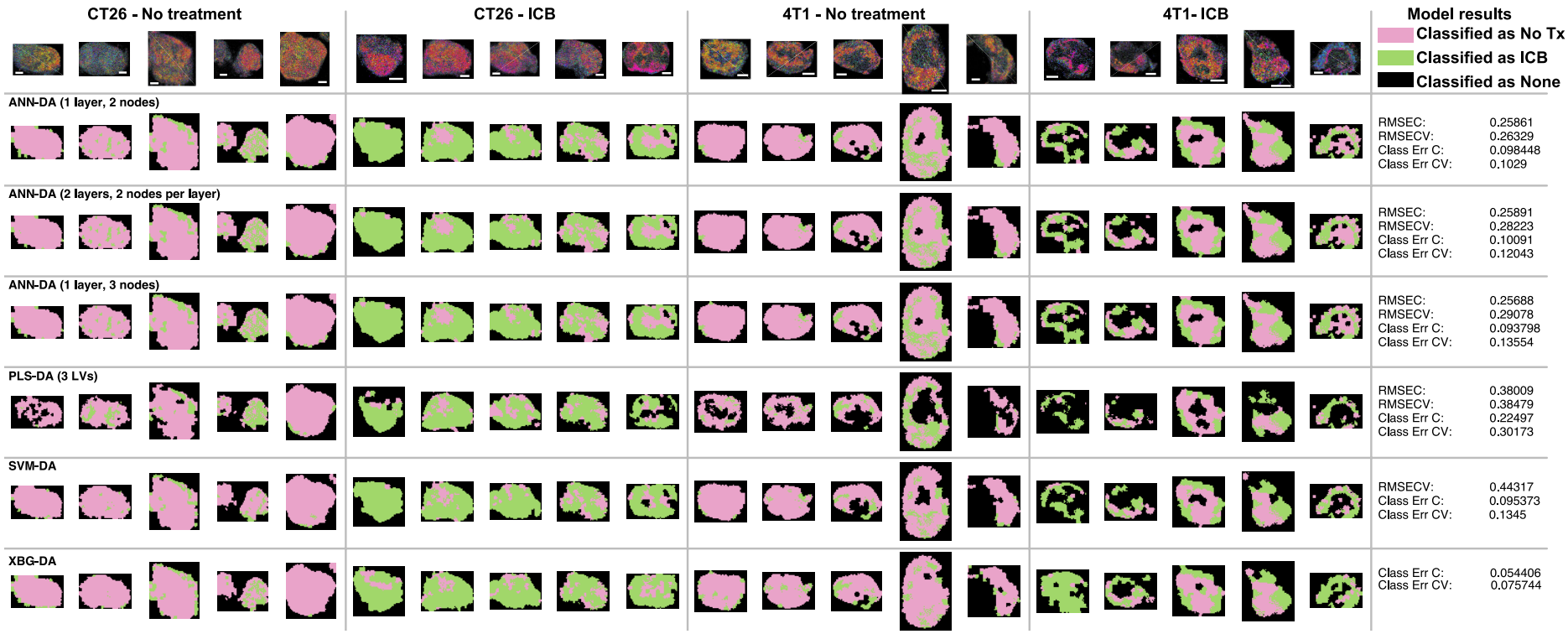

Figure S10. Supervised Machine Learning assessment. Several SML methods were used to classify the superpixels into "Treated" (ICB), "Not treated" (No Tx), and "No tumor" (None) groups. The methods performed comparably, classifying most superpixels correctly, independent of the tumor type (CT26 or 4T1). Areas that appear misclassified demonstrate uptake characteristics more similar to the other group, or low signal leading to a 'None' classification. This stems from intratumoral variations and may signify tumor areas with increased or suppressed immune activity. ANN, artificial neural network; DA, discriminant analysis; PLS, partial least squares; LV, latent variable; SVM, support vector machines; XBG, boosted gradient trees.

Table S1. Commercial IR and custom ChPIR dyes used for SERS nanoprobe synthesis

Dye name	Empirical formula	Counterion	Total MW	Volume for synthesis (μl dye 20 mM in DMF /ml of IPA)
IR780p	$C_{37}H_{37}ClN_2O_4$	ClO_4	609.15	6
IR140	$C_{39}H_{34}Cl_3N_3O_4S_2$	ClO_4	779.19	6
IR820	$C_{46}H_{50}ClN_2NaO_6S_2$	N/A	849.47	6
IR783	$C_{38}H_{46}ClN_2NaO_6S_2$	N/A	749.35	8
IR797	$C_{31}H_{34}Cl_2N_2$	Cl	505.52	1.5
IR775	$C_{32}H_{36}Cl_2N_2$	Cl	519.55	2
IR780i	$C_{36}H_{44}ClIN_2$	I	667.11	1.5
IR792	$C_{42}H_{49}ClN_2O_4S$	ClO_4	713.37	6
ChPIR-779	$C_{29}H_{19}S_6$	PF_6	704.79	2
ChPIR-820$_3$	$C_{29}H_{19}S_4Se_2$	PF_6	798.59	2
ChPIR-813	$C_{29}H_{19}S_6$	PF_6	704.79	1
ChPIR-825	$C_{29}H_{19}S_2Se_4$	PF_6	892.39	0.25
ChPIR-870	$C_{29}H_{19}Se_6$	PF_6	986.19	0.5
ChPIR-846$_3$	$C_{29}H_{19}S_2SeTe$	PF_6	795.21	6
ChPIR-794	$C_{27}H_{24}NS_3$	PF_6	603.64	6
ChPIR-820$_2$	$C_{27}H_{24}NS_2Se$	PF_6	650.54	2
ChPIR-817	$C_{25}H_{22}NS_3$	PF_6	577.60	2
ChPIR-853	$C_{25}H_{22}NS_2Se$	PF_6	624.50	2
ChPIR-820$_4$	$C_{25}H_{22}NSSe_2$	PF_6	671.40	1
ChPIR-863	$C_{25}H_{22}NSe_3$	PF_6	718.30	0.5
ChPIR-728	$C_{23}H_{20}NS_3$	PF_6	551.56	10
ChPIR-761	$C_{23}H_{20}NS_2Se$	PF_6	598.46	10
ChPIR-732	$C_{23}H_{20}NSSe_2$	PF_6	645.36	1
ChPIR-768	$C_{23}H_{20}NSe_3$	PF_6	692.26	2
ChPIR-868	$C_{36}H_{50}ClO_2$	BF_4	695.20	6
ChPIR-904	$C_{34}H_{46}O_2Se_2$	N/A	644.66	30
ChPIR-846$_5$	$C_{32}H_{42}O_2Se_2$	N/A	616.61	6
ChPIR-814	$C_{32}H_{42}O_2S_2$	N/A	522.81	30

Table S2. Antibodies used for nanoprobe functionalization and immunohistochemical validation

Target	Raman reporter	NP functionalization		IHC validation			
		Clone	Supplier	Host species	Supplier	Product number	Concentration (μg/ml)
CD8	**IR140**	2.43	BioXCell	Rabbit	Cell Signal	98941	2.4
GITR	**ChPIR-794**	DTA-1	BioXCell	Goat	R&D systems	AF524	1
4-1BB	**ChPIR-728**	3H3	BioXCell	Goat	R&D systems	AF937	0.5
CD11b	**IR780p**	M1/70	BioXCell	Rabbit	AbCam	Ab133357	1
NKp46	**IR820**	29A1.4	eBioscience	Goat	R&D systems	AF2225	2
CD4	**IR797**	YTS177	BioXCell	Goat	R&D systems	AF554	2
PD-L1	**ChPIR-825**	B7-H1	eBioscience	Goat	R&D systems	AF1019	2
IgG control	**IR820**	RG7/11.1	BioXCell	Goat	Santa Cruz	SC2028	2× [primary]
				Rabbit	Invitrogen	10500C	2× [primary]

References

1. Harmsen, S.; Bedics, M. A.; Wall, M. A.; Huang, R.; Detty, M. R.; Kircher, M. F., Rational design of a chalcogenopyrylium-based surface-enhanced resonance Raman scattering nanoprobe with attomolar sensitivity. *Nat Commun* **2015,** *6*, 6570.
2. Bedics, M. A.; Kearns, H.; Cox, J. M.; Mabbott, S.; Ali, F.; Shand, N. C.; Faulds, K.; Benedict, J. B.; Graham, D.; Detty, M. R., Extreme red shifted SERS nanotags. *Chem Sci* **2015,** *6* (4), 2302-2306.
3. Detty, M. R.; McKelvey, J. M.; Luss, H. R., Tellurapyrylium dyes. 2. The electron-donating properties of the chalcogen atoms to the chalcogenapyrylium nuclei and their radical dications, neutral radicals, and anions. *Organometallics* **1988,** *7* (5), 1131-1147.
4. Detty, M. R.; Henne, B., Squarylium Dyes Based on 2,6-Di-Tert-Butylselenopyrylium or Telluropyrylium Nuclei. *Heterocycles* **1993,** *35* (2), 1149-1156.
5. Balaban, T., AT Balaban Pyrylium salts. *Science of synthesis: Houben–Weyl methods of molecular transformations, EJ Thomas, Ed., Thieme, Stuttgart* **2003,** *14*, 11-200.